ISSN: 2447-3359

REVISTA DE GEOCIÊNCIAS DO NORDESTE

Northeast Geosciences Journal

v. 12, nº 2 (2026)

https://doi.org/10.21680/2447-3359.2026v12n2ID37875

Evaluation of the expansive and collapsible potential of soils from the Jandaíra Formation: A case study in an urbanized area in Mossoró – RN

Avaliação do potencial expansivo e colapsível de solos da Formação Jandaíra: Um estudo numa área urbanizada de Mossoró – RN

Bianca Alencar Vieira[1]; Olavo Francisco dos Santos Júnior[2]; Osvaldo de Freitas Neto[3]; Ricardo Nascimento Flores Severo[4]

[1] Federal Rural University of the Semi-Arid Region, Department of Engineering, Caraúbas, Rio Grande do Norte, Brazil. Email:bianca.vieira@ufersa.edu.br
ORCID: https://orcid.org/0000-0001-8306-2781

[2] Federal University of Rio Grande do Norte, Department of Civil and Environmental Engineering, Natal, Rio Grande do Norte, Brazil. Email: olavo.santos@ufrn.edu.br
ORCID: https://orcid.org/0000-0001-7552-6646

[3] Federal University of Rio Grande do Norte, Department of Civil and Environmental Engineering, Natal, Rio Grande do Norte, Brazil. Email: osvaldocivil@ufrn.edu.br
ORCID: https://orcid.org/0000-0001-9488-4123

[4] Federal Institute of Education, Science and Technology of Rio Grande do Norte, Academic Directorate of Civil Construction, Natal, Rio Grande do Norte, Brazil. Email: ricardo.severo@ifrn.edu.br
ORCID: https://orcid.org/0000-0001-9568-860X

Resumo: Understanding the behavior of unsaturated soils is essential in geotechnical engineering, particularly in semiarid regions, where climatic conditions favor the development of potentially collapsible and expansive soils. This study investigates the behavior of soils susceptible to swelling and/or collapse in the Mossoró region, Rio Grande do Norte State, within the Jandaíra Formation. A geotechnical investigation program was carried out, including laboratory tests for physical characterization, swelling, collapse, and shear strength assessment, as well as field investigations consisting of Standard Penetration Tests (SPT) and hand-auger borings. The results revealed soils predominantly classified as clayey sand, with high penetration resistance. Some samples exhibited expansive behavior, particularly compacted specimens prepared from the fine soil fraction, which developed high swelling pressures, whereas others showed collapse upon inundation. The direct shear test results indicated behavior typical of sandy soils with a high fines content, characterized by a pronounced peak shear strength and high apparent cohesion at peak conditions. After failure, cohesion decreased significantly, while the friction angle remained practically unchanged.

Keywords: Geotechnical investigation; Unsaturated soils; Semi-arid region.

Abstract: A compreensão de solos não saturados é essencial na engenharia geotécnica, especialmente em regiões semiáridas, onde as condições climáticas favorecem a formação de solos potencialmente colapsíveis e expansivos. Este estudo investiga o comportamento de solos suscetíveis à expansão e/ou colapso na região de Mossoró – RN, inserida na Formação Jandaíra. Para tanto, realizou-se uma investigação geotécnica através de ensaios de laboratório, incluindo caracterização física, ensaios de expansão, colapso e resistência ao cisalhamento dos solos, e ensaios de campo, especificamente sondagens à percussão (SPT) e à trado. Os resultados revelaram solos predominantemente classificados como areia argilosa e com alta resistência à penetração. Algumas amostras apresentaram comportamento expansivo, principalmente em amostras compactadas com a fração fina do solo, com elevadas tensões de expansão, enquanto outras exibiram colapso sob inundação. A avaliação do ensaio de cisalhamento direto mostrou um comportamento típico de solos arenosos com alta fração fina, com resistência de pico bem acentuada e alta coesão antes do cisalhamento, que foi significativamente reduzida após a ruptura, mantendo-se o ângulo de atrito praticamente inalterado.

Palavras-chave: Investigação geotécnica; Solos não saturados; Região semiárida.

Recebido: 03/10/2024; Aceito: 08/05/2025; Publicado: 14/08/2026.

1. Introduction

Soil, as the essential foundation for all engineering structures, plays a role that extends beyond its structural function, serving as a crucial construction material. However, the presence of expansive and/or collapsible soils represents a major concern, posing serious challenges to the safety and performance of engineering works, as well as causing substantial economic losses.

In several regions of Brazil, clayey, unsaturated, and highly porous soils are commonly found. The behavior of these soils with respect to their swelling and collapse potential has been widely investigated. For example, Ferreira and Ferreira (2009) evaluated, through oedometer tests conducted under different conditions, the changes in soil volume and swelling pressure resulting from variations in water content in a Vertisol from the municipality of Petrolândia, Pernambuco State. In another study, Barbosa *et al.* (2022) characterized an expansive soil located in southwestern Amazonia. In turn, Barbosa, Marques, and Guimarães (2023) proposed a simplified method for assessing the swelling potential of clays based on geotechnical physical characterization tests. The proposed method is based on the correlation between the plasticity index (PI) and the silt/clay content.

Falcão *et al*. (2023) analyzed the collapse potential of a soil located in the state of Rio Grande do Sul. The main results showed that shear strength was strongly associated with soil suction. In addition, pile load tests revealed a significant reduction in bearing capacity attributed to the saturation of previously unsaturated soils. Bandeira *et al*. (2024) investigated the behavior of a soil from the municipality of Juazeiro do Norte, Ceará State, under inundation, with a focus on its application to shallow foundations. The undisturbed soil exhibited collapsible behavior upon wetting. In contrast, the compacted soil showed a significant reduction in collapse settlement.

The Brazilian semiarid region is characterized by a climate marked by prolonged drought periods and scarce, irregular rainfall. These climatic conditions result in a distinctive hydrological regime, with high evapotranspiration rates and low rates of water infiltration into the soil, favoring the formation of unsaturated soils with potential for collapse and swelling.

The Brazilian semiarid region is characterized by prolonged drought periods and scarce, irregular rainfall. These climatic conditions result in a distinctive hydrological regime, with high evapotranspiration rates and limited water infiltration into the soil, favoring the development of unsaturated soils with potential for collapse and swelling.

Some studies have identified expansive clay minerals, such as smectite and vermiculite, in the composition of carbonate soils developed in regions affected by water deficit, particularly under semiarid climatic conditions (HU *et al*., 2021; AL-AHBASHI; DAFALLA, 2023). In the Jandaíra Formation, Lemos and Curi (1997) and Oliveira *et al*. (2018) also reported the presence of these clay minerals in the fine fraction of soils developed over limestones of this geological formation.

Although the Jandaíra Formation covers a large portion of the territory of Rio Grande do Norte State, the literature on the geotechnical characterization of soils in this region remains limited. The relevance of this study lies in the need for a more detailed understanding of the geotechnical characteristics of soils developed from the Jandaíra Formation. This is particularly important in view of increasing urbanization and the expansion of industrial sectors, such as renewable energy production, exemplified by the widespread development of wind farms throughout the state.

Given this context, this study aims to analyze the behavior of soils susceptible to swelling and/or collapse in the Mossoro region, Rio Grande do Norte State, within the Jandaíra Formation. To this end, a geotechnical investigation program was carried out, including field and laboratory tests, in an area of the municipality where residential buildings exhibited significant signs of distress, possibly associated with soil swelling and/or collapse.

2. Methodology

2.1. Study area

The study area is located in the municipality of Mossoro, in the state of Rio Grande do Norte, Brazil. The municipality covers a total area of 2,099.3 km², making it the largest municipality in the state in terms of territorial extent (IBGE, 2023). Mossoro is situated in a region characterized by a very hot semiarid climate. Dry conditions predominate for approximately 7 to 8 months of the year, from June to January, whereas the rainy season extends from February to May, corresponding to the wet period (SGB, 2014; IDEMA, 2008).

In addition, the municipality of Mossoro is geographically located within the Potiguar Basin. Its geological framework comprises several lithostratigraphic units, among which the Jandaíra Formation is particularly prominent, covering a large portion of the municipality, as shown in Figure 1. It should be noted that the sampling sites are located within this geological unit. Regarding the pedological characteristics of the study area, the samples were collected in a region classified as Dystrophic Yellow Latosol, according to Santos *et al*. (2011). Several residential buildings in this area exhibited signs of distress possibly associated with soil swelling and shrinkage. These manifestations included fissures and cracks in masonry elements, as well as differential displacements between the raft foundations and the foundation soil.

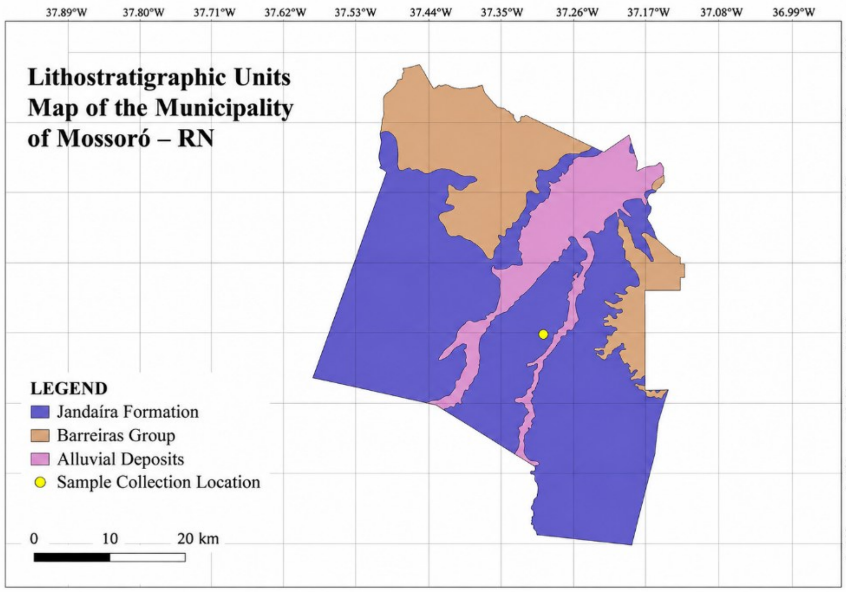

Figure 1 – Map of the lithostratigraphic units of the municipality of Mossoro.
Source: Authors; Geological Survey of Brazil (2024).

2.2. Field investigation

To determine the subsurface profiles and assess the in-situ penetration resistance of the soils, thirteen Standard Penetration Tests (SPT) with water circulation were performed, in addition to twenty hand-auger borings. Figure 2 shows the distribution of the boreholes and the locations where undisturbed samples were collected within the study area.

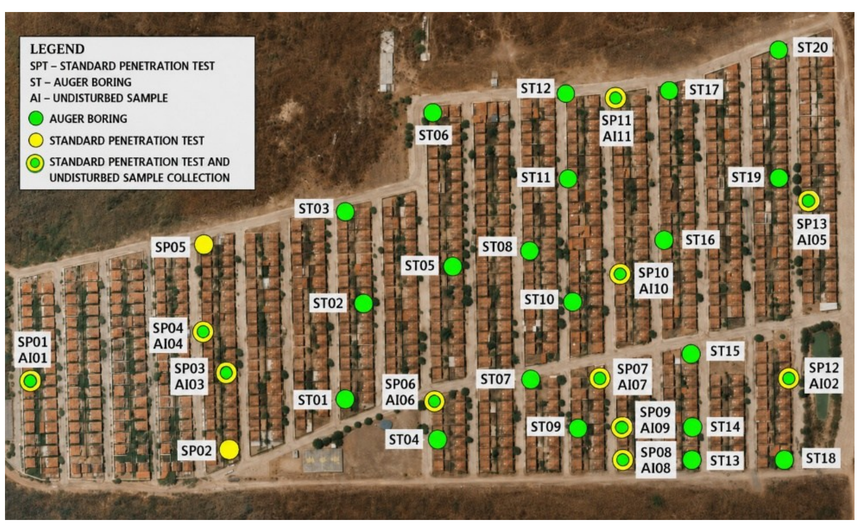

Figure 2 – Location of sampling points and boreholes.
Source: Authors (2024).

In addition, to better understand the vertical distribution of the soils, an inspection pit was excavated adjacent to hand-auger borehole ST 10 to a depth of 0.90 m. Below this depth, the investigation continued by hand augering to 1.50 m. Disturbed soil samples were collected at different depths below the ground surface, specifically at 0.20 m, 0.60 m, 0.80 m, 1.00 m, 1.40 m, and 1.50 m. The inspection pit allowed the identification of distinct soil layers, including gravelly, sandy, and clayey soils. The gravel particles exhibited smooth, rounded to subrounded surfaces, typical of pebbles, with diameters greater than 2 mm.

2.3. Laboratory investigation

Physical characterization tests were performed on eleven undisturbed samples collected at a depth of 0.50 m, whose locations are shown in Figure 2, as well as on the six disturbed samples obtained from hand-auger borehole ST 10. These tests included particle-size distribution analysis, following the procedures established in ABNT NBR 7181:2016; determination of the Atterberg limits, in accordance with ABNT NBR 6459:2016 and NBR 7180:2016; and determination of the specific gravity of soil solids, according to ABNT NBR 6458:2016. The Standard Proctor compaction test, in accordance with NBR 7182:2016, and the direct shear test were performed on the sample with the highest swelling potential, namely sample AI 03. In addition, swelling tests were conducted on all undisturbed samples, whereas collapse tests were performed on the samples that exhibited collapsible potential.

2.3.1. Expansibility tests

Free swell tests were conducted using conventional oedometer cells, following the procedures specified in ASTM D4546-21. For these tests, the specimens were prepared in stainless-steel rings measuring 19.00 mm in height and 50.3 mm in diameter.

Undisturbed specimens were prepared from samples AI 01, AI 02, AI 03, AI 04, AI 07, AI 08, AI 10, and AI 11. In contrast, remolded specimens were prepared from samples AI 01, AI 03, AI 05, AI 06, and AI 09. For the preparation of the remolded specimens, the soil fraction previously air-dried and passing the No. 10 sieve (2.0 mm) was used. The soil was statically compacted directly into the metal ring, reaching an average dry density of 2.0 g/cm³.

Free swell tests were conducted using conventional oedometer cells in accordance with the procedures specified in ASTM D4546-21. The specimens were prepared in stainless-steel rings measuring 19.00 mm in height and 50.3 mm in diameter.

Undisturbed specimens were obtained from samples AI 01, AI 02, AI 03, AI 04, AI 07, AI 08, AI 10, and AI 11. Remolded specimens, in turn, were prepared from samples AI 01, AI 03, AI 05, AI 06, and AI 09. For the preparation of the remolded specimens, the soil was previously air-dried and the fraction passing the No. 10 sieve (2.0 mm) was used. The soil was then statically compacted into the metal ring to an average density of 2.0 g/cm³.

The specimens were inundated under a surcharge pressure of 7 kPa. Soil deformation was monitored until stabilization was reached. After the swelling had stabilized, each specimen was subjected to incremental loading stages until it returned to its initial height. The stress required to restore the specimen to its initial height was defined as the swelling pressure.

2.3.2. Collapsibility tests

Collapse tests were performed to evaluate the soil collapse potential using conventional oedometer cells, following the procedures specified in ASTM D5333-3. The specimens were prepared in stainless-steel rings measuring 19.0 mm in height and 50.3 mm in diameter.

Undisturbed specimens were obtained from samples AI 02, AI 04, AI 07, AI 08, AI 10, and AI 11, based on the significant vertical compressive deformation observed during the inundation stage of the swelling tests. Each specimen was subjected to incremental compressive stresses of 12.5 kPa, 25 kPa, and 50 kPa. Inundation was performed after the application of the 50 kPa stress and stabilization of the axial deformation. After inundation, changes in specimen height were monitored until deformation stabilization was reached.

Based on the results obtained, the soil collapse index was calculated in accordance with ASTM D5333-03. The collapse index represents the vertical deformation of the soil resulting from inundation under an applied stress and is given by Equation 1:

$$I_C\ (\%) = \frac{\Delta h}{h_0} \times 100 \quad (1)$$

Where:
I_C (%) is the collapse index;
Δh s the change in specimen height due to inundation;
h_0 is the initial specimen height.

2.3.3. Direct Shear Tests

Direct shear tests were performed to determine the soil shear strength parameters under inundated and consolidated conditions for sample AI 03, in accordance with ASTM D3080/D3080M-23. For specimen preparation, remolded soil passing the No. 4 sieve (4.8 mm) was statically compacted into metal molds measuring 31.8 mm in height and 59.4 mm in diameter, at the optimum moisture content and maximum dry density. The direct shear tests were conducted at a constant displacement rate of 0.025 mm/min under three different normal stresses of 50, 100, and 200 kPa to evaluate the shear response of the soil.

3. Results and Discussion

3.1. Physical Characterization of the Soils

Table 1 summarizes the particle-size distribution results for the analyzed soils. Most samples are predominantly sandy, while also containing a considerable clay fraction. According to the Unified Soil Classification System (USCS), the soils were predominantly classified as clayey sand (SC). In addition, a significant gravel fraction was identified in some samples, particularly AI 01 and AI 05. Based on both field and laboratory observations, these gravel particles exhibited smooth, rounded, and/or subrounded surfaces, which are characteristic of pebbles.

Based on the samples obtained from hand-auger borehole ST 10 and the associated inspection pit, the gravel layer was found at a shallow depth, ranging from 0.60 to 0.80 m below the ground surface. It should be noted that the occurrence of gravel at such shallow depths may be related, at least in part, to previous anthropogenic activities, such as earthworks, disposal of construction and demolition waste, or uncontrolled urban development.

Table 1 – Particle-size distribution of the soils.

Sample	Particle-size distribution						USCS
	Gravel	Coarse sand	Medium sand	Fine sand	Silt	Clay	
AI - 01	29.59%	11.42%	10.62%	6.70%	8.96%	32.71%	GC
AI - 02	8.45%	18.26%	24.67%	12.45%	6.17%	30.01%	SC
AI - 03	20.31%	8.79%	20.71%	18.13%	10.44%	21.63%	SC
AI - 04	18.65%	13.79%	17.18%	11.91%	10.9%	27.57%	SC
AI - 05	30.83%	15.15%	20.84%	10.48%	5.97%	16.73%	SC
AI - 06	13.98%	14.62%	24.09%	14.56%	6.61%	26.14%	SC
AI - 07	21.62%	12.35%	19.02%	11.26%	8.66%	27.10%	SC
AI - 08	20.70%	14.87%	34.86%	16.59%	3.61%	9.37%	SC
AI - 09	22.75%	22.14%	18.01%	4.47%	6.99%	25.65%	SC
AI - 10	18.22%	12.04%	13.28%	13.91%	9.71%	32.84%	CH
AI - 11	13.99%	12.63%	19.06%	13.59%	12.02%	28.70%	SC
ST 10 – 0,2 m	11.26%	20.78%	22.12%	13.35%	7.84%	26.65%	SC
ST 10 – 0,6 m	46.59%	15.42%	17.49%	9.52%	3.52%	7.45%	GM
ST 10 – 0,8 m	49.00%	8.70%	12.12%	7.55%	6.04%	16.60%	GC
ST 10 – 1,0 m	7.57%	16.41%	28.17%	21.80%	9.33%	16.72%	SC
ST 10 – 1,4 m	13.76%	19.37%	24.65%	13.28%	3.69%	25.25%	SC
ST 10 – 1,5 m	14.55%	17.62%	24.45%	15.56%	5.02%	22.81%	SC

Source: Authors (2024).

Table 2 presents the results of the consistency limits, density of soil solids, water content, and clay activity tests for the analyzed soils. The density of soil solids ranged from 2.53 to 2.75 g/cm³. In addition, the fine fraction of nearly all samples was classified as having medium to high plasticity according to the classification criterion proposed by Burmister (1949).

Table 2 – Results of the consistency limits, density of soil solids, and water content tests.

Sample	Consistency			Density of soil solids (g/cm³)	Water content (%)
	LL (%)	LP (%)	IP (%)		
AI - 01	52.79	28.80	23.99	2.75	10.58
AI - 02	45.80	16.46	29.34	2.73	7.31
AI - 03	28.01	12.81	15.19	2.66	6.78
AI - 04	39.10	18.86	20.24	2.72	7.79
AI - 05	24.92	17.68	7.24	2.70	3.81
AI - 06	32.67	19.72	12.95	2.71	4.59
AI - 07	32.70	17.73	14.97	2.82	7.93
AI - 08	18.48	NP	-	2.71	3.40
AI - 09	38.13	20.26	17.87	2.72	5.20
AI - 10	60.26	26.68	33.57	2.74	10.15
AI - 11	41.38	25.09	16.28	2.77	7.79
ST 10 – 0,2m	30.26	15.62	14.64	2.67	3.66
ST 10 – 0,6m	17.67	13.76	3.91	2.68	1.69
ST 10 – 0,8m	36.70	19.67	17.03	2.72	4.90
ST 10 – 1,0m	23.44	14.09	9.35	2.75	2.55
ST 10 – 1,4m	34.43	23.37	11.06	2.70	3.95
ST 10 – 1,5m	35.21	19.91	15.31	2.71	3.45

LL = Liquid Limit; PL = Plastic Limit; PI = Plasticity Index.
Source: Authors (2024).

Among the indirect methods used to assess the swelling potential of soils, the criterion proposed by Van der Merwe (1964) is noteworthy, as it relates the clay fraction percentage and the soil plasticity index (PI) to its swelling potential. Most of the soil samples analyzed can be classified as having a swelling degree ranging from medium to very high, as indicated by the green cross in Figure 3.

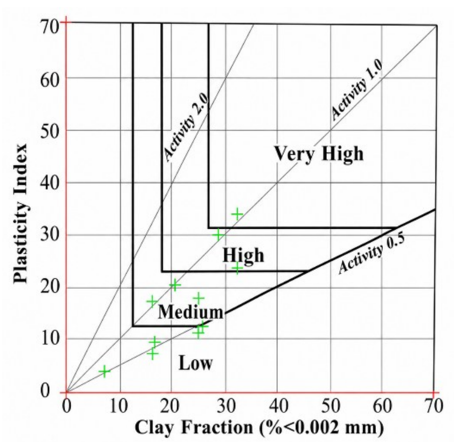

Figure 3 – Van der Merwe chart.
Source: Authors (2024).

The compaction curve for sample AI 03, shown in Figure 4, indicated a maximum dry density of 1.63 g/cm³ at an optimum moisture content of 22.9%. The maximum dry density value falls within the expected range for clayey sands. However, the optimum moisture content, which is higher than the typical range for this type of soil (generally between 8% and 15%), suggests a relatively high clay fraction, estimated at approximately 21% based on the particle-size distribution analysis. This behavior may be attributed to the significant clay content, particularly if expansive clay minerals are present. Soils with high clay contents generally require greater amounts of water to reach their maximum dry density due to their high water-retention capacity and tendency to swell.

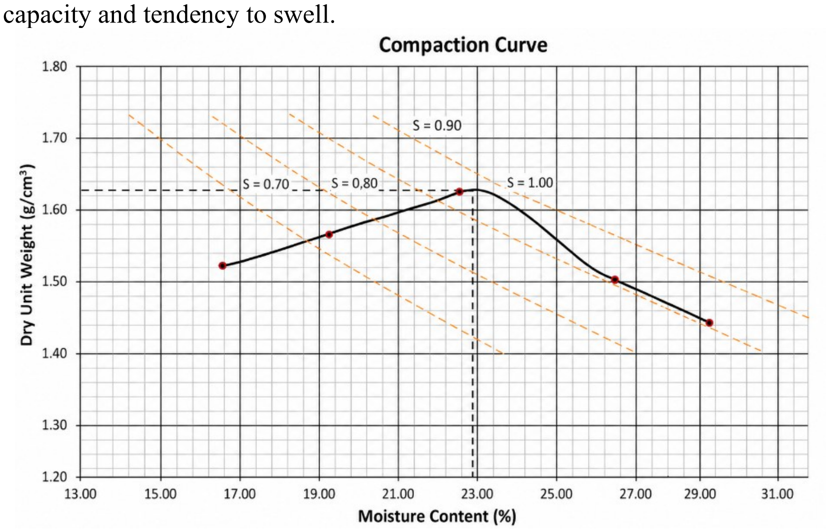

Figure 4 – Compaction curve for sample AI 03.
Source: Authors (2024).

3.2. Penetration Resistance and Geotechnical Subsurface Profiles

Analysis of the SPT results indicated high soil penetration resistance at the investigated locations, as shown in Table 3, which presents the obtained N_{SPT} values. The boreholes reached an average depth of 1.45 m, except at SP 01, where drilling advanced to 2.45 m before being terminated due to refusal of the wash boring tool, in accordance with the termination criteria established by ABNT NBR 6484:2020.

Table 3 – Results of the Standard Penetration Tests (SPT).

Borehole	Initial test depth (m)	N_{SPT}	Visual-tactile soil description	Relative density
SP 01	1.0	19	Gravelly sand	Dense
	2.0	23	Gravelly silty-clayey sand	Dense
SP 02	1.0	30	Gravelly clayey sand	Dense
SP 03	1.0	25	Gravelly clayey sand	Dense
SP 04	1.0	4	Gravelly clayey sand	Loose
SP 05	1.0	30	Gravelly clayey sand	Dense
SP 06	1.0	30	Gravelly clayey sand	Dense
SP 07	1.0	16	Gravel	-
SP 08	1.0	35	Gravelly clayey sand	Dense
SP 09	1.0	7	Gravelly clayey sand	Loose
SP 10	1.0	55	Gravelly clayey-silty sand	Very dense
SP 11	1.0	30	Gravelly clayey-silty sand	Dense
SP 12	1.0	30	Gravelly clayey sand	Dense
SP 13	1.0	30	Gravelly clayey sand	Dense

Source: Authors (2024).

Most of the soil samples collected during the borehole investigations were classified, based on visual-tactile examination, as dense clayey sand with gravel. This classification was corroborated by the particle-size distribution analyses performed in the laboratory for nearly all samples, showing good agreement with the field observations. The high clay content of the soil, combined with the low moisture conditions typical of the dry season during which the tests were carried out (August), may have contributed to the increased penetration resistance. In unsaturated soils, a reduction in water content may increase matric suction and, consequently, the apparent strength of the soil, contributing to the high N_{SPT} values observed during the tests.

Based on the SPT boreholes, two geotechnical subsurface profiles were developed, as shown in Figure 5. Profile 1 was drawn transverse to the study area, whereas Profile 2 was defined along its longitudinal direction. An impenetrable layer was encountered at a relatively shallow depth, approximately 1.50 m below the ground surface. This condition may be attributed to two possible factors: (i) the presence of limestone rocks of the Jandaíra Formation, which cropped out at some borehole locations; and (ii) the occurrence of a gravel layer at shallow depths, ranging from 0.60 to 1.00 m below the ground surface, as also observed in the inspection pit. These factors may account for the penetration difficulties encountered during the investigation and should be considered in the geotechnical assessment of the study area.

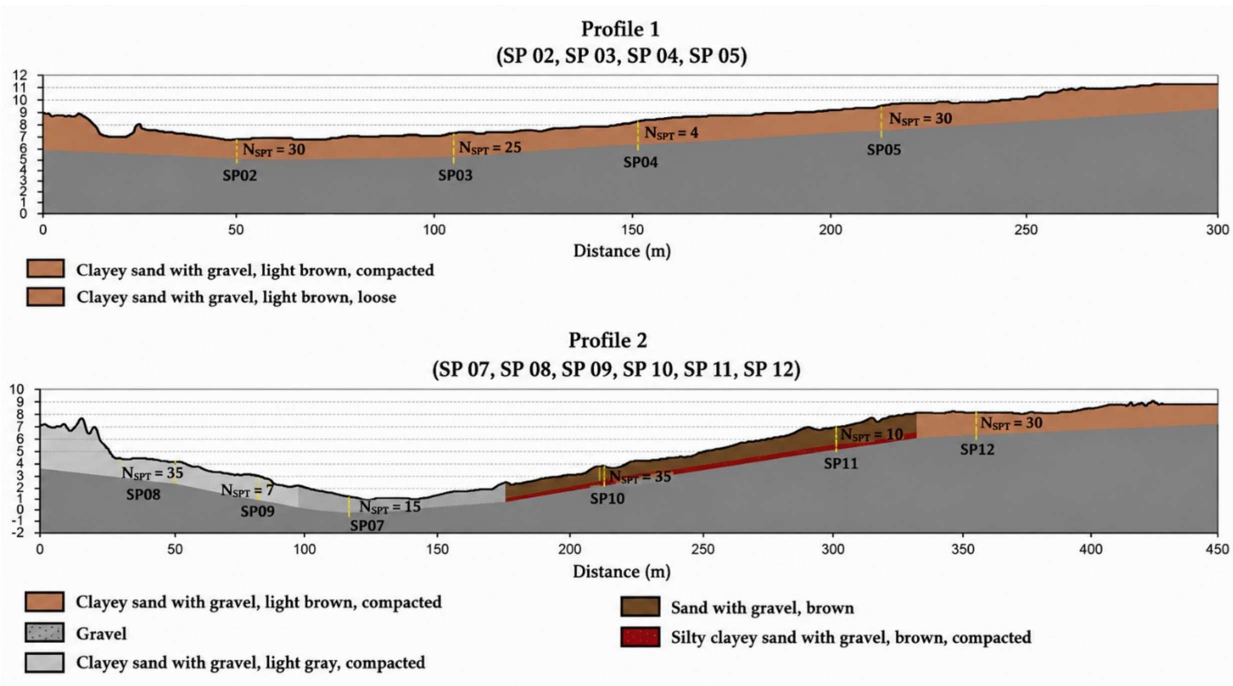

Figure 5 – Geotechnical subsurface profiles.
Source: Authors (2024).

Although the impenetrable layer occurs at a relatively shallow depth, the foundations adopted for the residential buildings consist of rigid concrete raft foundations. These raft foundations are placed directly on the surficial soil layer, which, due to its unsaturated condition and high clay content, is susceptible to significant volumetric changes when exposed to variations in moisture content, particularly during periods of intense rainfall. Such changes may adversely affect foundation performance. Because the residential buildings are relatively small, they impose comparatively low loads on the foundation soil. However, upon wetting or saturation, the soil may undergo swelling and/or collapse, resulting in differential settlements of the foundation.

The hand-auger boreholes reached variable depths, ranging from 0.20 to 1.83 m. In general, most of the soil samples obtained from these boreholes were classified as clayey sand with gravel, in agreement with the results obtained from the SPT boreholes. The groundwater table was encountered only at borehole ST 10 and, after stabilization, was recorded at a depth of 1.50 m below the ground surface.

3.3. Evaluation of Swelling Potential

In the context of swelling tests, it is essential to analyze specimen behavior during the inundation stage in order to better understand the soil deformation characteristics. Figure 6 presents the plots of vertical strain versus the square root of time obtained during the inundation stage of the swelling tests performed on undisturbed specimens. The specimens obtained from samples AI 01 and AI 03 exhibited slight swelling, requiring a period of deformation stabilization before proceeding to the next loading stage. The swelling pressures obtained for samples AI 01 and AI 03 were 12.5 kPa and 10 kPa, respectively.

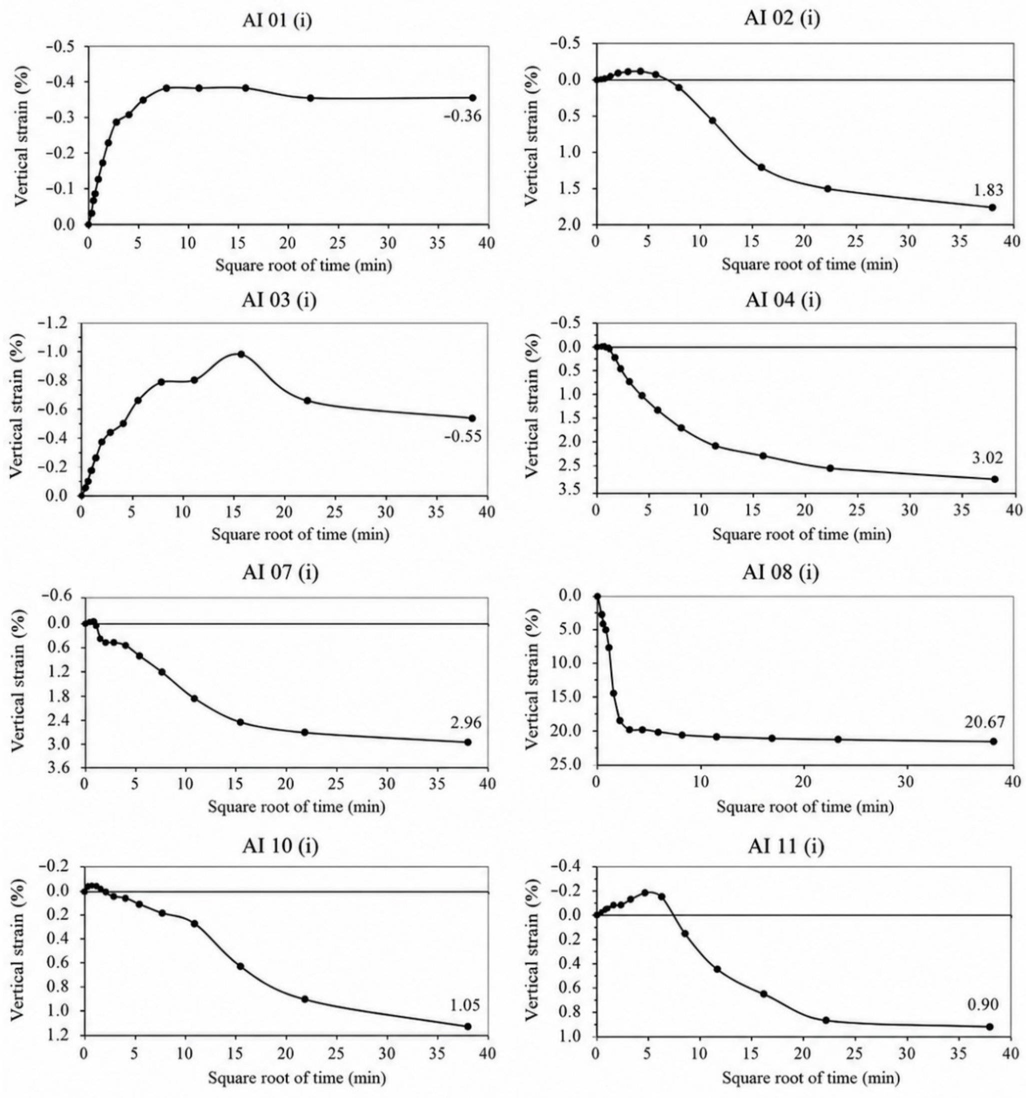

Figure 6 – Results obtained from the swelling tests on undisturbed samples.
Source: Authors (2024).

In contrast, the specimens obtained from samples AI 02, AI 10, and AI 11 initially exhibited a tendency to swell during the inundation stage; however, unlike samples AI 01 and AI 03, they returned to their initial height without requiring any additional increase in loading. It is noteworthy that, except for samples AI 01 and AI 03, the remaining soil samples exhibited a tendency to collapse when subjected to inundation, with vertical strain values ranging from 0.9% to 20.67% among the analyzed specimens.

Figure 7 presents the plots of vertical strain versus the square root of time obtained during the inundation stage of the swelling tests performed on remolded specimens. Significant swelling was observed when the specimens were prepared using the finer soil fraction. The resulting vertical strains ranged from 4.42% to 23.14% among the analyzed samples.

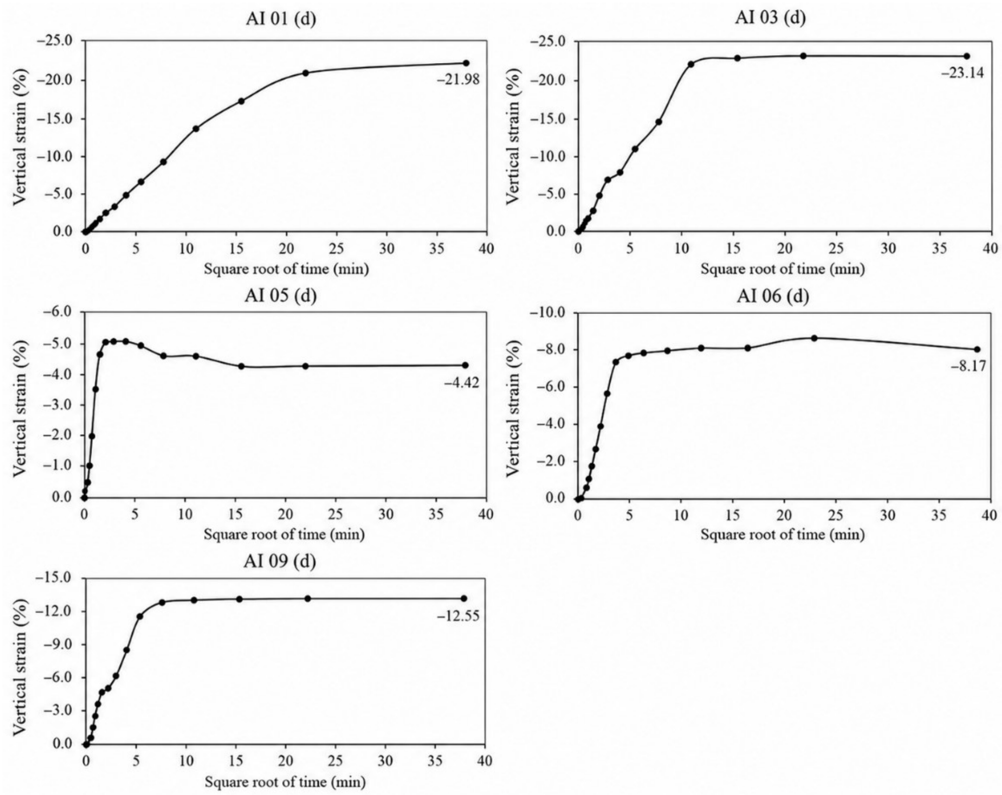

Figure 7 – Results obtained from the swelling tests on disturbed samples.
Source: Authors (2024).

In addition, the swelling pressures reached considerably higher values during the tests. Swelling pressures of 100 kPa were recorded for the specimens prepared from samples AI 05 (d) and AI 06 (d), 400 kPa for the specimens prepared from samples AI 03 (d) and AI 09 (d), and 800 kPa for sample AI 01 (d), as shown in Figure 8. The figure illustrates the stress–vertical strain behavior of the remolded specimens. Specifically, comparison of samples AI 01 (d) and AI 03 (d) under undisturbed and remolded conditions shows a marked increase in vertical strain due to swelling.

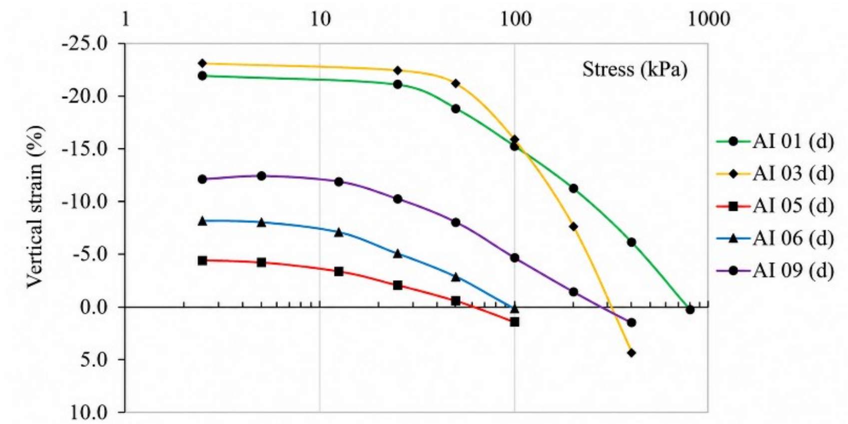

Figure 8 – Swelling curves of the disturbed specimens.
Source: Authors (2024).

3.4. Evaluation of Collapse Potential

In the study of soil collapsibility properties, it is essential to understand the evolution of vertical strain during inundation under an applied load. Figure 9 presents the graphs with the strains until reaching the inundation stress (50 kPa) of the specimens. The increments in vertical strain (Δεv) observed at the end of the inundation stage ranged from 0.65% to 9.58% in the analyzed samples, indicating different degrees of collapsibility among the soils. The smallest strain increment was observed in sample AI 02, with Δεv of 0.65%, and the largest reached 9.58% for sample AI 08.

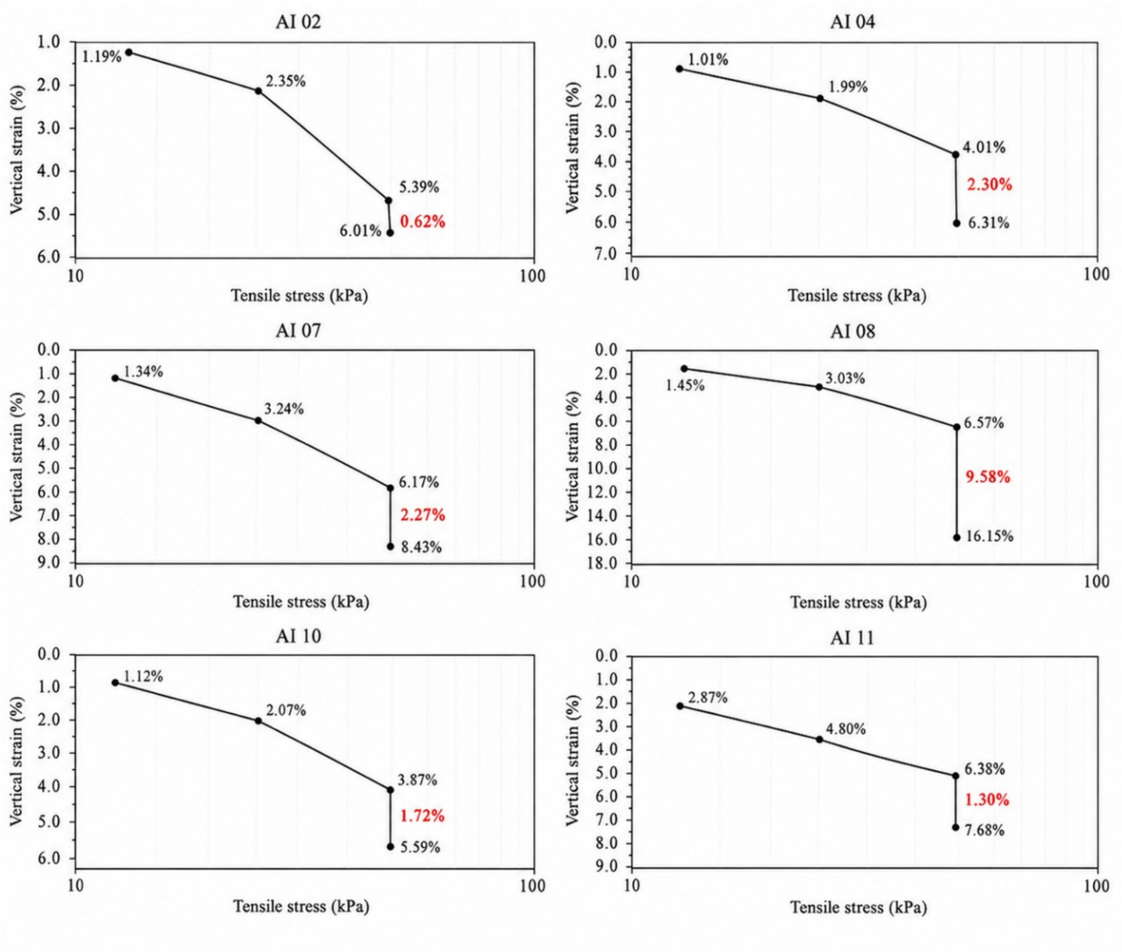

Figure 9 – Collapse curves with inundation at 50 kPa.
Source: Authors (2024).

The variation in vertical strain for samples AI 04, AI 07, and AI 08, under a stress of 50 kPa at the time of inundation, was greater than 2%. Therefore, according to the criterion proposed by Vargas (1977), these soils may be considered collapsible. On the other hand, based on the collapse index defined by Equation (1), sample AI 08 is classified as exhibiting moderately severe collapse according to ASTM D5333-03, whereas samples AI 04 and AI 07 are classified as exhibiting moderate collapse, and samples AI 02, AI 10, and AI 11 as exhibiting slight collapse.

It is important to highlight that, although the vertical strain of sample AI 10 was slightly lower than 2%, reaching 1.72%, its relevance should not be underestimated. Although it does not reach the threshold established by Vargas (1977) for classification as a collapsible soil and is classified as exhibiting slight collapse according to ASTM D5333-03, special attention should be given to this sample. This is due to the significant 44.44% variation in vertical strain observed during the inundation period, between the initial time (0 h) and the subsequent 24 h.

3.5. Soil Shear Strength

Direct shear tests were performed on sample AI 03, which exhibited the highest swelling potential. The specimens were subjected to normal stresses of 50, 100, and 200 kPa. Figure 10 shows the relationship between shear stress and horizontal displacement. It can be observed that, regardless of the applied stress, the soil exhibited a typical behavior, initially reaching a maximum, or peak, shear strength condition (strain-hardening phase), followed by a gradual decrease (strain-softening phase) until reaching the residual shear strength. This behavior is characteristic of soils with a high clay fraction, such as sample AI 03, which contains 21.63% clay, directly influencing the development of shear strength and the subsequent softening after the peak.

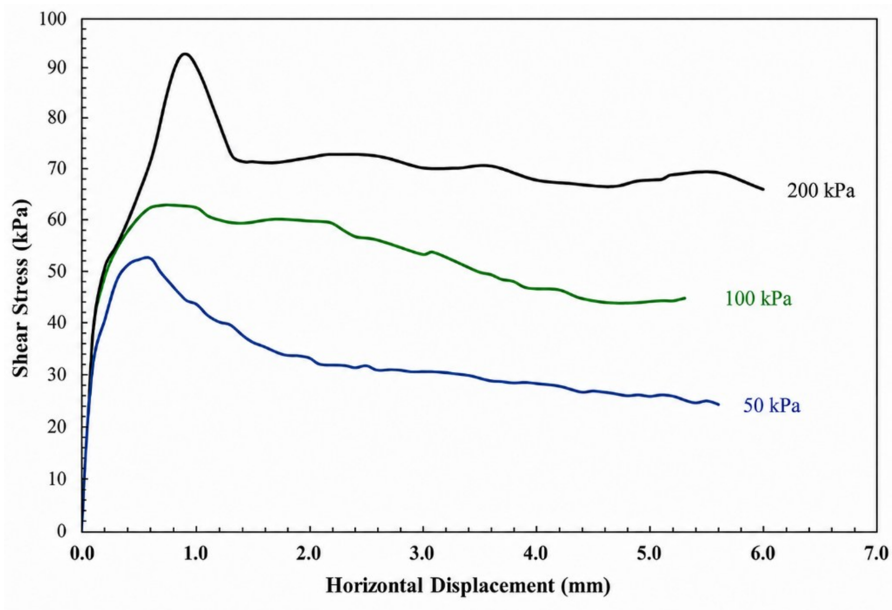

Figure 10 – Shear stress versus horizontal displacement for the direct shear test performed on sample AI 03. Source: Authors (2024).

Additionally, the peak strength is more pronounced under the highest applied normal stress, 200 kPa, for which the shear stress reached approximately 90 kPa. This behavior is expected due to the interlocking of soil particles, which increases with the application of higher normal stresses. When higher normal stresses are applied, the soil particles become more tightly packed, resulting in more effective confinement and, consequently, greater resistance to sliding between particles. This increase in particle interlocking leads to a higher peak shear strength, which explains the increase in shear stress as the normal stress increases.

Figure 11 presents the shear strength envelopes for both the peak and residual conditions, obtained under normal stresses of 50, 100, and 200 kPa. The peak envelope indicates a higher initial shear strength of the soil, with a cohesion of approximately 37.6 kPa and a friction angle of 15.04°. However, after the soil reaches its maximum strength and undergoes structural changes during shearing, the residual envelope indicates a significant reduction, with cohesion decreasing to approximately 14.2 kPa and the friction angle decreasing slightly to 14.73°. This behavior highlights the transition between the initial condition and the permanent deformation condition of the soil.

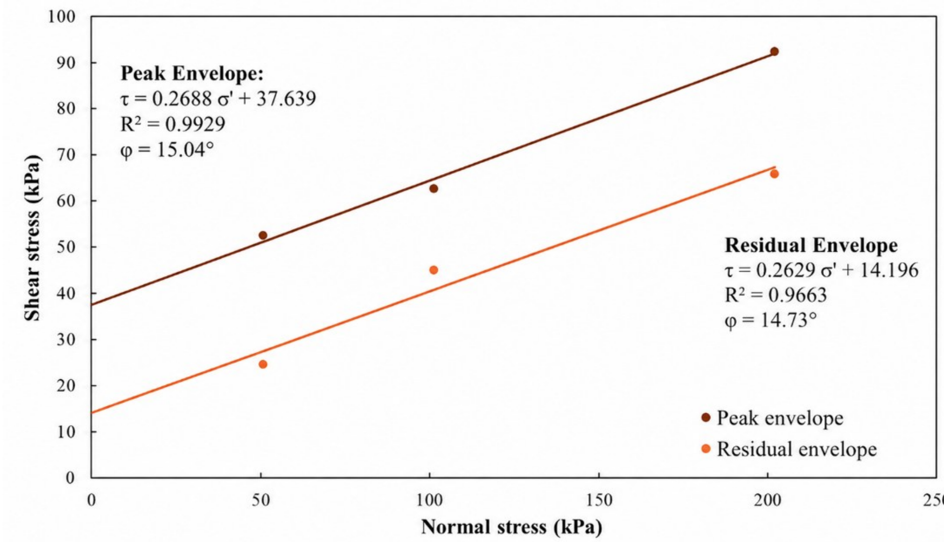

Figure 11 – Peak and residual shear strength envelopes for sample AI 03.
Source: Authors (2024).

In contrast, the soil friction angle shows little variation between the peak and residual conditions. With very similar values (15.04° and 14.73°, respectively), this small difference suggests that the internal friction between soil particles is not highly sensitive to the structural changes induced by shearing. Unlike cohesion, which decreases considerably, the friction angle remains nearly unchanged, indicating that the friction between the sand and silt particles present in the soil composition continues to contribute consistently to the shear strength, even after rearrangement of the soil structure.

4. Conclusions

This article presented a study on the behavior of soils susceptible to swelling and/or collapse in the Mossoró region, Rio Grande do Norte State, within the Jandaíra Formation, based on laboratory and field geotechnical tests. Based on the results obtained, the following conclusions can be drawn:

- The physical characterization indicated predominantly sandy soils with a significant clay fraction, classified as clayey sand (SC), with gravel occurring at shallow depths between 0.6 and 0.8 m below the ground surface.
- The compaction analysis of the sample with the highest swelling potential indicated a maximum dry density of 1.63 g/cm³ and an optimum moisture content of 22.9%, reflecting the presence of a significant clay fraction, with greater water-retention capacity and susceptibility to swelling.
- Analysis of the SPT results indicated high soil penetration resistance, which may be associated with low moisture conditions and a high clay fraction. Most of the samples were classified as dense clayey sand with gravel, corroborating the physical characterization results obtained in the laboratory.
- The soil profiles developed from the SPT boreholes indicated the presence of an impenetrable layer at an average depth of 1.50 m, associated with the occurrence of limestone outcrops or gravel.
- The swelling tests showed that only two undisturbed samples exhibited slight swelling during the inundation stage, whereas the remaining undisturbed samples showed a tendency to collapse upon inundation, with vertical strains ranging from 0.9% to 20.67%.
- The swelling tests performed on disturbed specimens showed greater swelling, with vertical strains ranging from 4.42% to 23.14%. The swelling pressures reached high values, ranging from 100 kPa to 800 kPa, indicating a significant increase in swelling in the specimens compacted using the fine soil fraction.
- The collapsibility tests under an applied stress of 50 kPa showed a significant increase in vertical strain during inundation, with values ranging from 0.65% to 9.58%. Three of the analyzed samples were classified as collapsible soils according to the criterion proposed by Vargas (1977). According to ASTM D5333-03, one sample was classified as exhibiting moderately severe collapse, whereas two samples exhibited moderate collapse.

- The direct shear test performed on the sample with the highest swelling potential showed behavior typical of clayey soils, with a peak shear strength followed by strain softening. The peak strength increased with increasing applied normal stress. Cohesion was significantly affected by shearing, whereas the friction angle showed negligible variation.

Based on the results of this study, the importance of understanding the behavior of unsaturated soils, particularly carbonate soils in semiarid regions, such as those of the Jandaíra Formation, when subjected to inundation and drying cycles and service stresses, is evident. This understanding is essential for assessing the need for soil treatments to ensure foundation stability, prevent pathological manifestations, and guarantee the safety of buildings.

References

ABNT - ASSOCIAÇÃO BRASILEIRA DE NORMAS TÉCNICAS. *NBR 6459: Solo - Determinação do limite de liquidez*. Rio de Janeiro: ABNT, 2016.

ABNT - ASSOCIAÇÃO BRASILEIRA DE NORMAS TÉCNICAS. *NBR 7180: Solo - Determinação do limite de plasticidade*. Rio de Janeiro: ABNT, 2016.

ABNT - ASSOCIAÇÃO BRASILEIRA DE NORMAS TÉCNICAS. *NBR 7181: Solo - Análise granulométrica*. Rio de Janeiro: ABNT, 2016.

ABNT - ASSOCIAÇÃO BRASILEIRA DE NORMAS TÉCNICAS. *NBR 7182: Solo – Ensaio de compactação*. Rio de Janeiro: ABNT, 2016.

ABNT - ASSOCIAÇÃO BRASILEIRA DE NORMAS TÉCNICAS. *NBR 6458: Grãos de pedregulho retidos na peneira de abertura 4,8 mm - Determinação da massa específica, da massa específica aparente e da absorção de água*. Rio de Janeiro: ABNT, 2017.

AL-MAHBASHI, A. M.; DAFALLA, M. *The distribution and mineralogy of expansive clay in a semi-arid region*. *Arabian Journal of Geosciences*, v. 16, n. 4, 283, 2023.

ASTM - AMERICAN SOCIETY FOR TESTING AND MATERIALS. *D5333-03 - Standard Test Method for Measurement of Collapse Potential of Soils*. Pennsylvania, EUA: 2017.

ASTM - AMERICAN SOCIETY FOR TESTING AND MATERIALS. *D4546-21 - Standard Test Methods for One - Dimensional Swell or Collapse of Soils*. Pennsylvania, EUA: 2021.

ASTM - AMERICAN SOCIETY FOR TESTING AND MATERIALS. *D3080/D3080M-23 - Standard Test Method for Direct Shear Test of Soils Under Consolidated Drained Conditions*. Pennsylvania, EUA: 2023.

BANDEIRA, A. P. N.; DE SOUZA NETO, J. B.; COUTINHO, R. Q.; XAVIER, J. M.; CHAVES, A. M. M.; DA SILVA ALVES, V. L. Investigating the Collapsible Behavior of Sedimentary Soil in Shallow Foundations. *Geotechnical and Geological Engineering*, v. 42, n. 4, 2725-2743, 2024.

BARBOSA, V. H. R.; MARQUES, M. E. S.; GUIMARÃES, A. C. R.; CASTRO, C. D. Characterization of an expansive soil in southwest Brazilian amazon - Behavior of an expansive subgrade in a flexible pavement. In: *Advances in Transportation Geotechnics IV: Proceedings of the 4th International Conference on Transportation Geotechnics Volume 3*. Springer International Publishing, 323-335, 2022.

BARBOSA, V. H. R.; MARQUES, M. E. S.; GUIMARÃES, A. C. R. Predicting soil swelling potential using soil classification properties. *Geotechnical and Geological Engineering*, v. 41, n. 8, 4445-4457, 2023.

BURMISTER, D. M. Principles and techniques of soil identification. In*: Proceedings of Annual Highway Research Board Meeting. National Research Council*. 402-434.Washington, DC. 1949.

FALCÃO, P. R.; BARONI, M.; MASUTTI, G. C.; PINHEIRO, R. J. B.; DE FREITAS FAGUNDES, D. Assessment of the impact of inundation on the strength of a lateritic and collapsible soil. *Geotechnical and Geological Engineering*, v. 41, n. 8, 4761-4773, 2023.

FERREIRA, S. R. M.; FERREIRA, M. G. V. X. Mudanças de volume devido a variação de teor de umidade em um Vertisolo no Semi-Árido de Pernambuco. *Revista Brasileira de Ciência do Solo (Impresso)*, v. 33, n. 33, 779-791, 2009.

HU, J.; CI, E.; LI, S.; LIAN, M.; ZHONG, S. The pedogenesis of soil derived from carbonate rocks along a climosequence in a subtropical mountain, China. *Forests*, v. 12, n. 8, 1044, 2021.

IBGE - INSTITUTO BRASILEIRO DE GEOGRAFIA E ESTATÍSTICA. Mossoró - Panorama. Disponível em: https://cidades.ibge.gov.br/brasil/rn/mossoro/panorama. Acesso em: 05/07/2024.

IDEMA - INSTITUTO DE DESENVOLVIMENTO SUSTENTÁVEL E MEIO AMBIENTE. *Perfil do seu município - Mossoró*. Natal: IDEMA, 2008.

LEMOS, M. S. S; CURI, N. Evaluation of characteristics of Cambisols derived from limestone in low tablelands in northeastern Brazil. v. 32, n. 8. *Pesquisa Agropecuária Brasileira*, 825-834, 1997.

OLIVEIRA, D. P.; SARTOR, L. R.; JÚNIOR, V. S.; CORRÊA, M. M.; ROMERO, R. E.; ANDRADE, G. R. P.; FERREIRA, T. O. Weathering and clay formation in semi-arid calcareous soils from Northeastern Brazil. *Catena*, v. 162, 325–332, 2018.

SGB - SERVIÇO GEOLÓGICO DO BRASIL - CPRM. *Geologia e recursos minerais da folha Mossoró*. Recife: CPRM, 2014.

SANTOS, H. G.; CARVALHO JÚNIOR, W.; DART. R. O.; ÁGLIO, M. L. D.; SOUSA, J. S.; PARES, J. G.; FONTANA, A.; MARTINS, A. L. S.; OLIVEIRA, A. P. Sistema brasileiro de classificação de solos. Brasília - DF: Embrapa, 2018.

VAN DER MERWE D. H. The Prediction of Heave from Plasticity Index and Percentage Fraction of Soils. *Civil Engineer in South Africa*, 103–107, 1964.

VARGAS, M. *Introdução à Mecânica dos Solos*. São Paulo: Mcgraw-Hill, Editora da Universidade de São Paulo, 1977.